Constraints on the lunar core composition and thermal state from geophysical data and thermodynamic properties of liquid iron alloys

A. Rivoldini[(1)] [Attilio.Rivoldini@oma.be], M.-H. Deproost[(1,2)], and T. Van Hoolst[(1)]: [1] Observatoire Royal de Belgique, [2] KU Leuven, Leuven, Belgique

Introduction

A precise knowledge of thermodynamic properties of the lunar core is of prime importance for the ongoing efforts to reanalyze Apollo seismic data, for the interpretation of results from GRAIL and future projects to send seismometers to the lunar surface, and for understanding the thermal evolution of the Moon. Here we present a new coherent thermodynamic model for Fe-S alloys to infer the composition and present-day temperature of the lunar core from recent geodesy data by assuming a mantle density distribution deduced from lunar seismic data. Additionally we study the effects of the two models on the thermal evolution of the core and evaluate the core's capacity to generate a magnetic field.

Experimental data and thermodynamic model

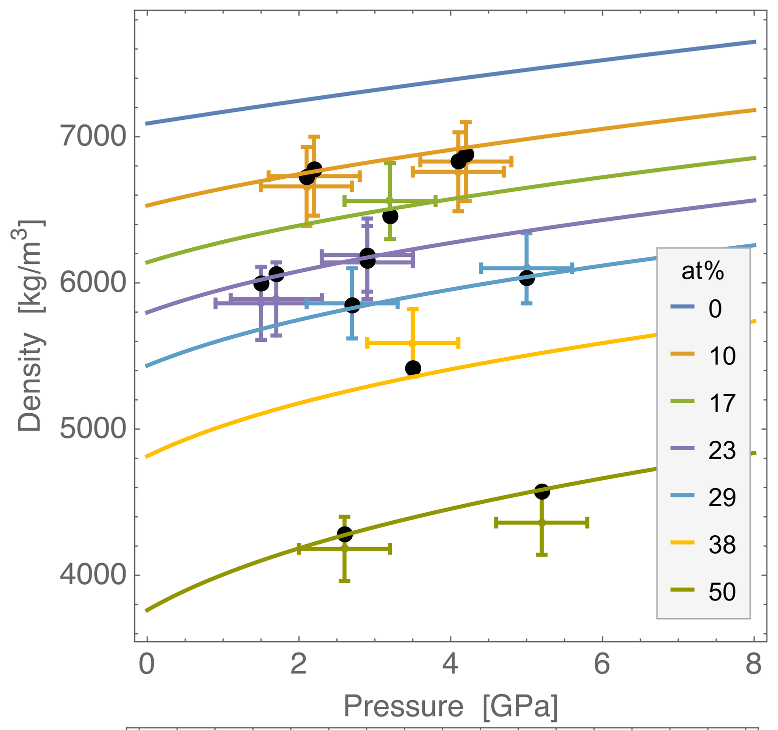

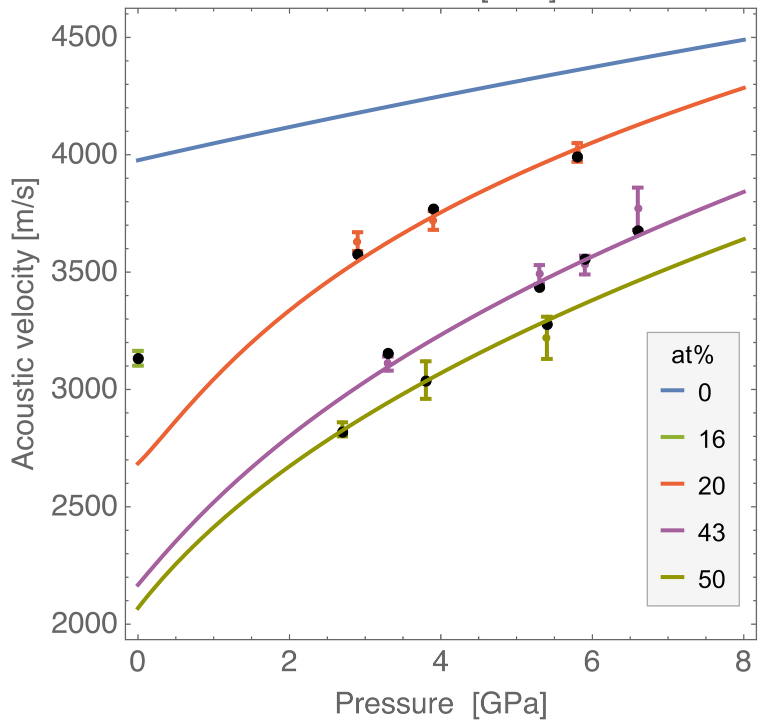

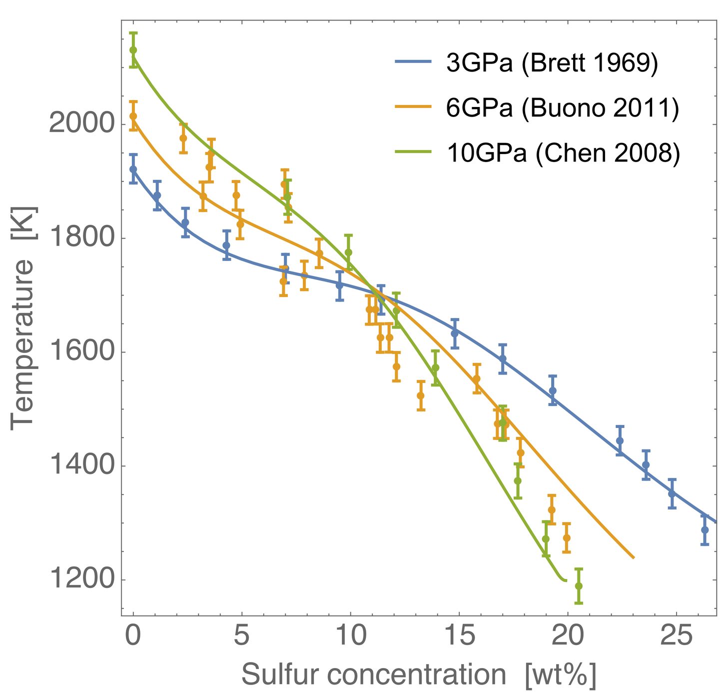

Data

- liquidus of Fe (Anzellini et al., 2013)
- iron-rich liquidus of Fe-S at 3 GPa, 6 GPa, and 10 GPa (Brett and Bell, 1969; Buono and Walker, 2011; Chen et al., 2008)
- equations of state for solid fcc Fe and l-Fe (Komabayashi, 2014)
- densities of liquid Fe-S alloys measured by X-Ray absorption (Morard et al., 2018)
- ambient pressure density of l-FeS (Kress, 2007) and ambient pressure sound velocity of l-Fe5wt%Ni10wt%S (Nasch et al., 1997)
- acoustic velocity data of liquid Fe-S alloys measured by ultrasonic pulse-echo method (Nishida et al., 2016)

Thermodynamic model

- iron-rich liquidus data of Fe-S between 3-10 GPa can be described with an asymmetric Margules model that has interaction parameters linear in pressure and temperature (Buono and Walker, 2011).
  The Gibbs free energy of the liquid is:

$$
\begin{aligned}
G^l(x,p,T) = &(1-x)\,G^l_{\mathrm{Fe}}(p,T) + x\,G^l_{\mathrm{FeS}}(p,T) + \\
&(1-x)\,R\,T\ln(1-x) + x\,R\,T\ln(x) + \\
&x(1-x)\left[x\,W_{\mathrm{Fe}}(p,T) + (1-x)\,W_{\mathrm{FeS}}(p,T)\right],
\end{aligned}
$$

  where R is the gas constant, x the molar fraction of FeS, G^l_i the Gibbs energy of the end-members and the W_i the interaction parameters
- this solution model induces a concentration dependent but pressure and temperature independent excessive mixing volume that can well summarize the high pressure density data but not the sound velocity data
- a pressure dependent excessive volume is required for the mixing model to agree with the liquidus, density, and sound velocity data

Thermodynamic model predictions

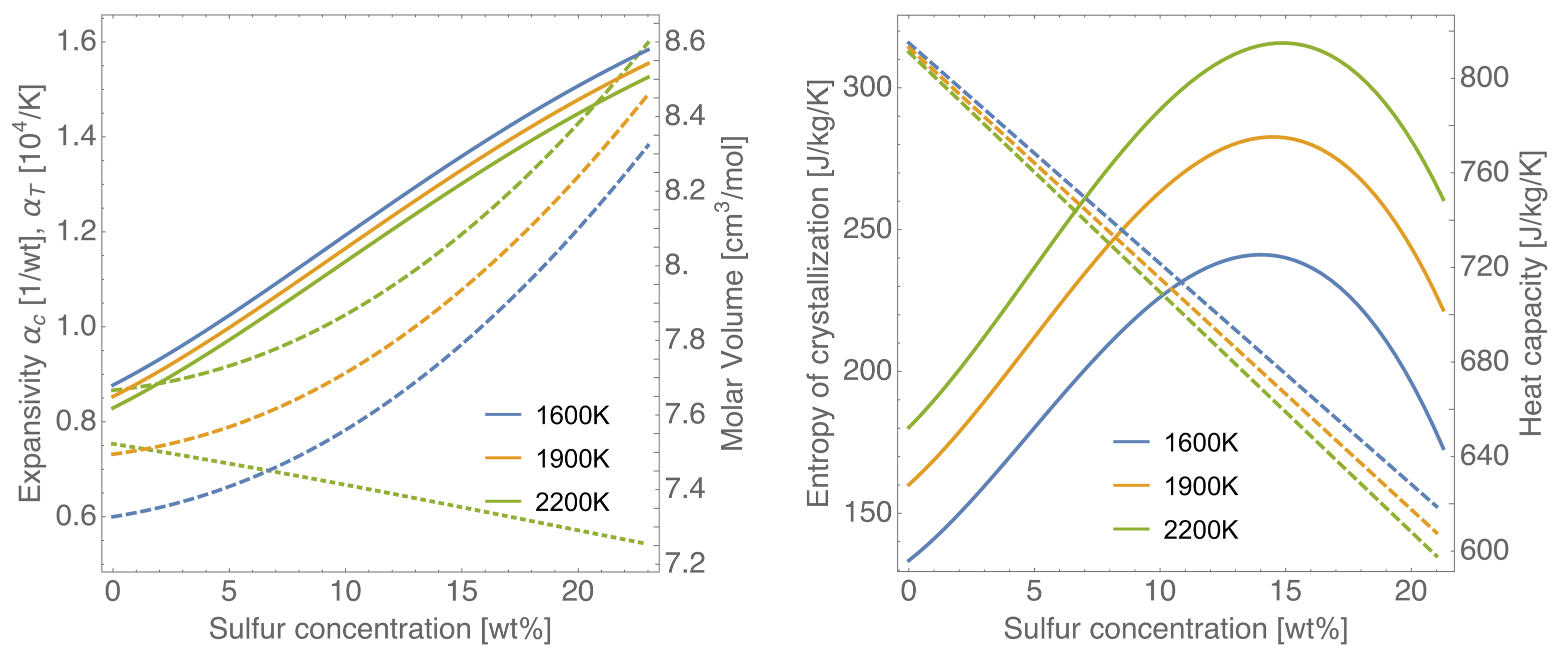

Left figure: Chemical expansivity α_c (full), thermal expansivity α_T (dotted), and molar volume (dashed) as a function of sulfur concentration at 6 GPa. **Right figure:** Entropy of crystallisation (full) and heat capacity at constant pressure (dashed) as a function of sulfur concentration at 6 GPa.

Moon model

- interior structure models agree with the latest estimate of the average moment of inertia of the silicate shell (MOIs $= 0.393112 \pm 0.000012$) (Williams et al., 2014)
- based on the mantle density model of Weber et al. (2011)
- core thermal evolution model based on Davies et al. (2015) and mantle evolution model based on Morschhauser et al. (2011)
- thermal conductivity depends on pressure, temperature, and sulfur concentration (Secco and Schloessin, 1989; Konôpková et al., 2016)

Structure Functions

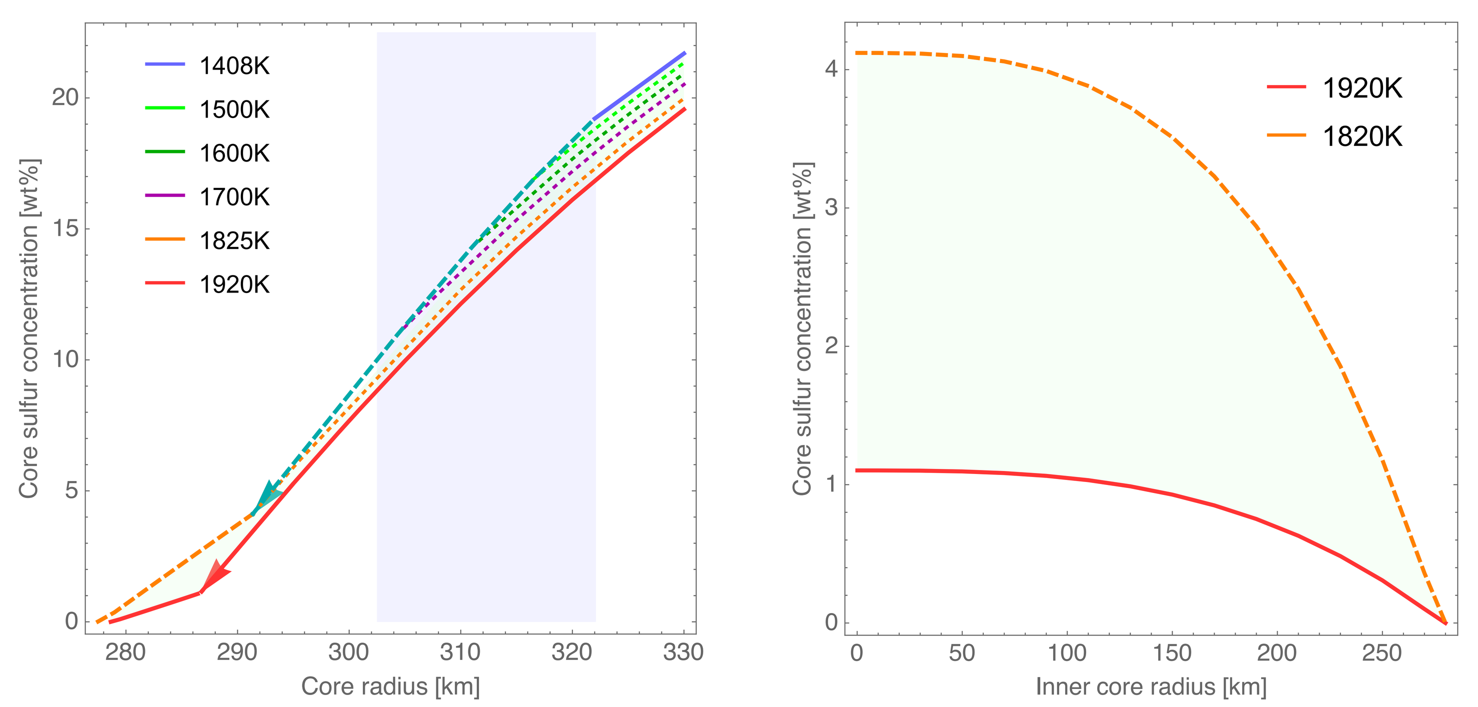

Core sulfur concentration as a function of core radius (left figure) and as a function of inner core radius (right figure). Models that are to the left of the arrowhead have an inner core and models on the dashed curves have iron-snow in their liquid core reaching down to the center of the planet or to the inner core boundary. Eventually triggering top-down inner core formation (not modeled here). Models in the blue shaded area agree with the MOIs at 1σ

→ for models to agree with the MOIs the core-mantle boundary temperature cannot be below 1408K ($x_S \lesssim$ 20wt%S)

→ to avoid lower mantle melting the core-mantle boundary temperature cannot be much larger than 1920K, i.e. below the peridotite solidus (Hirschmann et al., 2012)

→ models with the Weber et al. (2011) mantle density profile that agree with the MOIs at 1σ cannot have an inner core

Thermal evolution

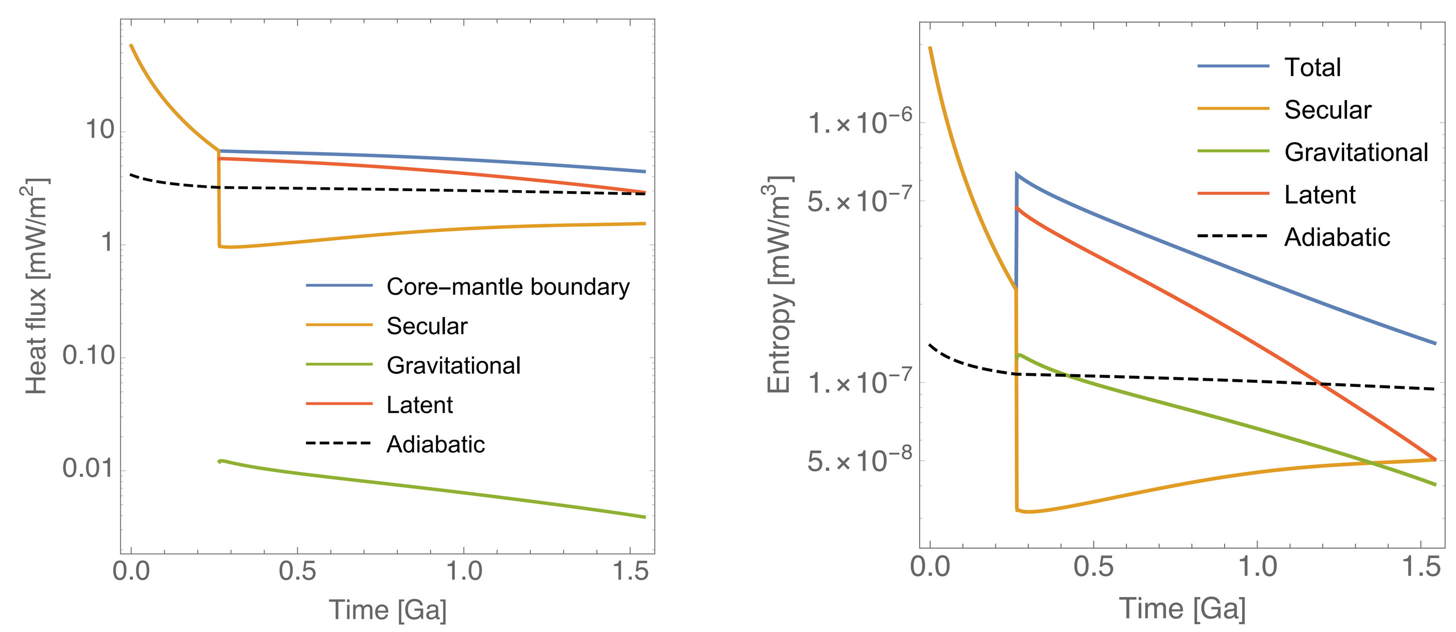

Heat flux (left) and entropy (right) evolution until iron snow reaches the inner core boundary, for a model with 1.63wt% of sulfur an initial core-mantle temperature of 2200K. The black dashed lines represent the heat and entropy transported along the adiabat at the core-mantle boundary. The total available power and entropy are shown by blue lines.

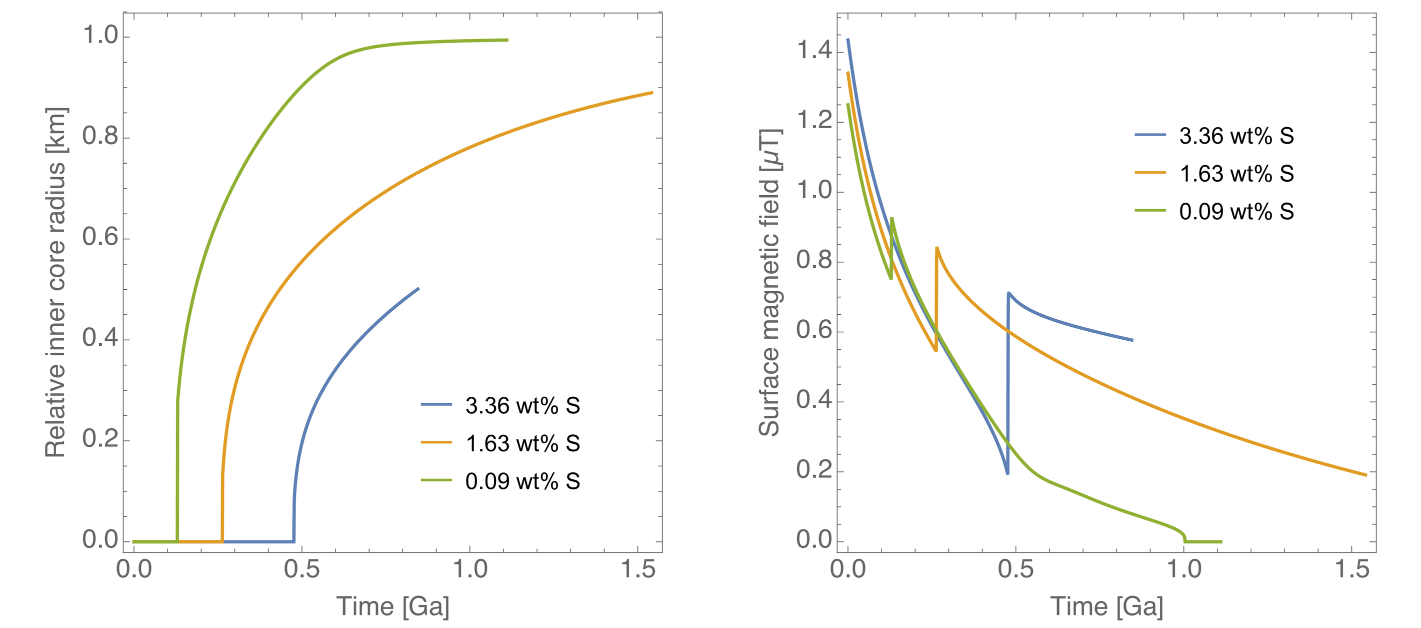

Evolution of relative inner core radius and surface magnetic field strength until iron snow reaches the inner core boundary, for models with an initial core-mantle boundary temperature of 2200K. The magnetic field strength is calculated from a scaling law (Aubert et al., 2009) using the entropy available for Ohmic dissipation.

Conclusion

- melting data and new elastic data about Fe-S alloys can be described with a non-ideal mixing model that has a pressure dependent excess volume
- to agree with the MOIs at 1σ the core-mantle boundary temperature cannot be below $\sim$ 1408K and to avoid lower mantle melting it has to be below $\sim$ 1910K
- models with an inner core and without a whole snowing liquid core cannot be much colder than $\sim$ 1825K and those models have less than $\sim$ 4.3wt% of sulfur
- models without an inner core having a marginal dynamo until about 3.56Gyr ago require core-mantle boundary temperatures significantly above the mantle solidus ($\gtrsim$ 2500K)
  → models without an inner core cannot generate a dynamo in agreement with observations
- models with an inner core can have mantle boundary temperatures below the mantle solidus 1Gyr after formation and agree with the timing of occurrence of the lunar dynamo, but the predicted magnetic fields have magnitudes that are significantly below what is expected to explain the lunar magnetic records (20μT-110μT) (Tikoo et al., 2017)

Acknowledgments

This work was financially supported by the Belgian PRODEX program managed by the ESA in collaboration with the Belgian Federal Science Policy Office and by the Belspo BRAIN-be program (BR/143/A2/COME-IN)